SUMMARY OF STOL GROUND VORTEX INVESTIGATION[*]

Michael L. Billet

Applied Research Laboratory

The Pennsylvania State University

and

Marvin M. Walters

Naval Air Development Center

List of Symbols

C_p	static pressure coefficient
D_j	inner diameter of jet
P_a	ambient pressure
P_o	maximum pressure in the impingement region
q_o	reference dynamic pressure, equal to $(P_o - P_a)$
V	velocity
V_j	velocity of jet at nozzle exit
V_o	reference velocity, equal to $\sqrt{\dfrac{2q_o}{\rho}}$
V	velocity at jet centerline
V_x	velocity in the x direction
V_z	velocity in the z direction
V_∞	wind tunnel velocity
Z_i	jet impingement point
Z_{le}	vortex maximum penetration point
Z_s	vortex separation point
$\lambda *$	reference jet-to-crossflow velocity ratio $= \dfrac{V_o}{V_\infty}$

Introduction

The impingement of a concentrated circular jet exhaust flow on a ground plane results in the formation of a wall jet which flows radially from the point of impingement along the ground surface. Forward motion of the jet source or the introduction of a counter-flowing freestream interacts with the wall jet to create a stagnation line and tends to roll the wall jet back on itself forming a horseshow-shaped ground vortex, as illustrated in Figures 1 and 2. Generally taking the shape of an ellipse whose major axis is aligned with the freestream flow the location of this stagnation line is dependent on the relative velocity of the freestream and wall jet flows and the injection angle of the jet exhaust into the freestream flow. The location of the vortex is nearly coincident with the stagnation line but at a height above the ground which is also a function of the relative velocities of the jet and freestream flows. When flow conditions are appropriate for its formation, this vortex is a major source of the induced flow in the near field.

An experimental facility has been developed in the 1.23 m (48-inch) wind tunnel of the Applied Research Laboratory at The Pennsylvania State University to model this ground vortex. The purpose of this facility is to study the affect of various parameters on the location and characteristics of a ground vortex.

Previous studies concerning this type of flow are few and very limited in scope. Colin and Olivari [1] have experimentally determined the location and established the elliptical shape of the vortex line for one nozzle height. In addition a dimensionless relationship was proposed between the vortex separation point and the ratio of wall jet velocity at the impingement point

to the cross flow velocity. Parameters such as the presence or absence of a boundary layer on the ground plane have also been shown to influence the location of the ground vortex [2,3]. A recent survey on ground effects and testing techniques is given by Kuhn [4].

A recent effort by Stewart and Kuhn [5] to develop a prediction method for STOL ground effects indicated the need to not only establish the location of the ground vortex as it varies with parameters but also the strength of the resulting vortex. As a result, an experimental investigation was conducted in the 1.23 m (48-inch) wind tunnel into the formation, stability and strength of the ground vortex for several flow parameters. The intent of this paper is to summarize the design of the facility, special instrumentation and results.

Experimental Facility

All tests were conducted in the subsonic wind tunnel. This facility is a closed-circuit, closed-jet wind tunnel with an octagonal test section which is 1.2 m (4.0 ft) across and is 4.9 m (16.0 ft) long. The test section velocity can be varied continuously up to 36.6 m/s (120 ft/sec) and honeycombs and screens in the settling sections reduces the turbulence level in the test section to be less than 0.10 percent of the free stream velocity.

A 76.2 mm (3.00-inch) diameter open-jet was fabricated and inserted through one side of the test section as shown in Figure 3. The jet features a 16.0 to 1.0 contraction ratio and is equipped with two wire mesh screens and a honeycomb to reduce turbulence. The 45.7 m/s (150 ft/sec) jet was powered by a variable speed 3.7 kW (5-hp) blower which injested air from the wind tunnel at a port far downstream from the test camber.

The test facility was formed by two vertically mounted 2.4 m (8.0 ft) long wooden panels with circular arc leading edges. The jet tube extended

152.4 mm (6.0 inches) through the center of one of the panels. The movable ground board shown in Figure 4 was designed to facilitate conducting the various phases of the test program. The ground board was located between horizontal ceiling and floor inserts and could be positioned at 1, 2, 3, 4, or 6 jet diameters from the jet exit plane. At each position it could be moved and flared to control the static pressure gradient due to the wall boundary layer growth. In addition, a slot was included on the ground board for boundary layer control. The ground board was also equipped with interchangeable .6 m x .9 m (2 ft x 3 ft) window inserts. Three windows were available for various phases of the test program, i.e., a glass with fluorescent mini-tufts, a glass window for LDV surveys, and a plexiglass window instrumented with static pressure taps.

Instrumentation

The jet velocity was monitored via 3.17 mm (0.125-inch) diameter kiel probe in the plenum section and a static pressure tap in the wall of the jet tube. The wind tunnel velocity was measured by a 3.17 mm (0.125-inch) diameter pitot-static probe mounted on the floor insert midway between the sidewalls outside of all wall boundary layers. For the wall-to-wall flow surveys a miniature five-hole probe [8] fabricated at ARL/PSU was utilized. In addition, this five-hole probe was also used to determine the mean velocity jet characteristics and a single element hot wire anemometer was used to determine the turbulence characteristics. It is important to note that the jet characteristics were determined with the ground plane removed and the wind tunnel separated at points A and B as annotated in Figure 3.

Flow visualization tests to locate the separation line and the forward extent of the recirculation bubble on the ground plane were conducted with a

large matrix of fluorescent mini-tufts on the ground plane. This technique which was originally developed by Crowder [8] and was extended by Stinebring and Treaster [9] uses extremely fine fluorescent monofilament fibers [(0.178 mm 0.007-inch diameter)]. These fibers are attached to the window by a tiny drop of cyano-acrylate glue and illuminated by an ultraviolet light source to map the flow.

The static pressure distribution on the ground plane was measured via window insert having static pressure taps. In all, 56 static pressure taps having 0.787 mm (0.031-inch) diameter holes were used as shown in Figure 5.

All pressures in this test program were measured with individual transducers which could be sampled electronically. The temperature of the test environment was determined with a temperature probe and recorded as one of the input channels. All data were acquired on-line via the VAX 11-782 computer system which permitted on-site graphic terminal display of the primary and reduced test parameters and later hard copy output of the selected data.

Details of the ground vortex velocity field were determined by a five-beam, three-component laser Doppler velocimeter system. The system measured three velocity components at the crossing of three green beams and two blue beams by collecting the light scattered by the seeded particles in the flow. Thermal Systems, Inc., optics with a four-watt Lexal Argon-Ion laser was mounted on a three-axis traverse as shown in Figure 6. The digital output of the three counter processors were processed in a VAX 11-782 computer. The computer produces histograms of the measured velocities and computes the statistics of the flow including the mean velocity and turbulence intensity.

Summary of Experimental Results

Jet Characteristics

Velocity surveys to measure jet characteristics were conducted at $x/D_j = 1.0$, 2.0, 3.0, 4.0, and 6.0 with $V_j = 45.7$ m/s (150 ft/sec) across its potential core. The axisymmetric velocity profiles obtained with a 5-hole probe are shown in Figure 7 for the vertical plane. The surveys in the horizontal plane are virtually identical since the jet is axisymmetric. Shown in Figure 8 are turbulence measurements acquired by using hot-wire anemometry at $x/D_j = 2.0$. The turbulence intensity at the centerline and at $x/D_j = 2.0$ was experimentally measured to be less than 2%. The impingement point of the jet on the ground plane depends on the jet-to-crossflow velocity ratio (V_∞/V_j) and ground plane position (x/D_j). The variation of the jet impingement point with ground plane position for various jet-to-crossflow velocity ratios is shown in Figure 9.

Test Chamber Characteristics

The ground board location relative to the ground vortex location was varied longitudinally so that the LDV surveys could be centered at a position approximately 101.6 mm (4-inches) downstream of the window's leading edge. Thus, wall-to-wall surveys were conducted with no jet flow at the five x/D_j locations and crossflow velocities of 4.6, 9.1, 13.7, and 18.3 m/s (15, 30, 45, and 60 ft/sec). The data for 18.3 m/s (60 ft/sec) and $x/D_j = 2.0$ are shown in Figure 10 and is representative of the other velocity and location data. It is important to note that these survey data were obtained with the boards flared as to minimize the pressure gradient, and as the data of Figure 10 indicates, a uniform pressure from wall to wall was achieved.

Ground Vortex Position

The window instrumented with the fluorescent minitufts was used to obtain a first-order measurement of the ground vortex location. Photographs such as shown in Figure 11 were utilized to obtain the location of the separation line and the leading edge of the recirculating region (Z_{le}) on the ground board as shown in Figures 12-15. Z_s and Z_{le} were measured from the impingement point of the jet. The summary of the vortex position data are shown in Figures 16 and 17. In addition, data from tests conducted at Rockwell [10] are also included in Figure 17 and are shown to be in very good agreement. Several of the Z_{le} values at $V_\infty/V_j = 0.3$ and 0.4 were no longer on the viewing window as indicated in Table 1 which tabulates the various vortex parameters for each flow condition. Vortex oscillations were also noted and were most pronounced at $V_\infty/V_j = 0.1$ and 0.2.

Colin and Olivari [1] derived a dimensionless relationship between the vortex separation point and the ratio of wall jet velocity at the impingement point to the cross flow velocity. This relationship was derived by assuming that the energy in the wall jet equals the energy in the cross flow at the point of separation and is

$$\frac{Z_s}{D_j} = 1.03 \; \lambda^{*0.9} \tag{1}$$

where Z_s = vortex separation point and λ = reference jet-to-cross flow velocity ratio. Using the ground plane pressure data recorded earlier, the vortex separation point (Z_s) was calculated by Equation (1). These values are compared to theoretical values and flow visualization in Figure 18. Very good agreement was found although the boundary layer on the ground plane varied from 12.7 to 95.2 mm (0.5 to 3.75 inches) for the present study.

Laser Doppler Velocimeter Data

The 3-component LDV was utilized to measure the vortex velocity field on the ground plane. Initially, the shape of the vortex was visualized by micron particulate as they pass through a laser-light sheet. Photographs indicate that the vortex appears to be nonsymmetrical. In addition, flow visualizations indicated that very few of the cross-flow seeded particulate appeared in the core of the vortex structure where as most of the jet seeded particulate appeared in the core. Additional flow visualization tests are planned to document these particle trajectories.

Traverses through the center region of the vortex are shown in Figures 19-21 for the case of V_α/V_j = 0.1, 0.2 and x/D_j = 3.0. Velocities in the wall jet region were measured to be approximately twice the velocities measured in the opposing cross-flow region. This result notes a nonuniform energy distribution as opposed to the classical free vortex shape.

Summary of Investigation

A test facility suitable for the study of the ground vortex resulting from a jet impinging on a ground board in the presence of a cross-flow has been developed. The aerodynamic characteristics of the test chamber and jet have been determined. Data on the ground plane static pressure distributions and flow patterns were obtained for many flow conditions. Experimental data have confirmed Colin and Olivaris model. LDV measurements of the ground vortex indicates a nonsymmetric velocity distribution. In addition, the velocity field appears to have oscillations.

The data reported in this paper represents only some of the test results. More detailed velocity data of the ground vortex are currently being obtained with the LDV system. In addition more tests are currently being planned to determine the influence of incoming ground board boundary layer on the vortex location and characterize the stability of the ground vortex.

References

[1] Abbott, W. A., "Studies of Flow Fields Created by Vertical and Inclined Jet When Stationary or Moving Over a Horizontal Surface," RAE CP No. 911, 1967.

[2] Colin, P. E. and Olivari, D., "The Impingement of a Circular Jet Normal to a Flat Surface With and Without a Crossflow," Von Karman Institute for Fluid Dynamics, Rhode-St. Genese Belgium, January 1969.

[3] Crowder, J. P., "Add Fluorescent Mini-Tufts to the Aerodynamicists Bag of Tricks," Astronautics and Aeronautics, Vol. 18, November 1980, pp. 54-56.

[4] Kuhn, R. E., "V/STOL and STOL Ground Effects and Test Techniques," NASA No. NAS2-11912, December 1984.

[5] Schwantes, E., "The Recirculation Flow Field of a VTOL Lifting Engine," NASA TT F-14912, June 1973.

[6] Stewart, V. E. adn Kuhn, R. E., "A Method for Estimating the Propulsion Induced Aerodynamic Characteristics of STOL Aircraft in Ground Effects," NADC-80226-60, April 1982.

[7] Steward, V. and Kuhn, R., "A Method for Estimating the Propulsion Induced Aerodynamic Characteristics of STOL Aircraft in Ground Effects," NADC Report No. 80226-60, Vol. 2, August 1983.

[8] Stinebring, D. R. and Treaster, A. L., "Water Tunnel Flow Visualization by the Use of Fluorescent Mini-Tufts, The Applied Research Laboratory, TM No. 83-24, March 1983.

[9] "Treaster, A. L. and Yocum, A. M., "The Calibration and Application of Five-Hole Probes," ISA Transactions, Vol. 18, No. 3, 1979, pp. 23-24.

TABLE 1. GROUND VORTEX DIMENSIONS

V_∞/V_j	Z_i/D_j	Z_s/D_j	Z_u/D_j
$X/D_j = 1.0$			
0.1	0.00	4.25	7.75
0.2	0.00	2.75	5.25
0.3	0.00	2.25	4.75
0.4	0.00	1.50	3.25
$X/D_j = 2.0$			
0.1	0.00	4.00	6.25
0.2	0.00	2.75	4.25
0.3	-0.25	1.50	2.75
0.4	-1.00	0.00	2.25
$X/D_j = 3.0$ [a]			
0.1	0.00	5.50	7.75
0.2	-0.75	2.00	3.75
0.3	-1.00	0.25	2.25
0.4	*****	*****	1.00
$X/D_j = 4.0$ [a]			
0.1	-0.50	5.75	8.25
0.2	-1.50	0.75	3.00
0.3	-2.75	*****	1.50
0.4	*****	*****	*****
$X/D_j = 6.0$ [a]			
0.1	-0.5	4.50	7.50
0.2	-3.25	-2.25	1.75
0.3	*****	*****	*****
0.4	*****	*****	*****

[a] ***** indicates that the ground vortex was blown downstream off of the tuft window.

217
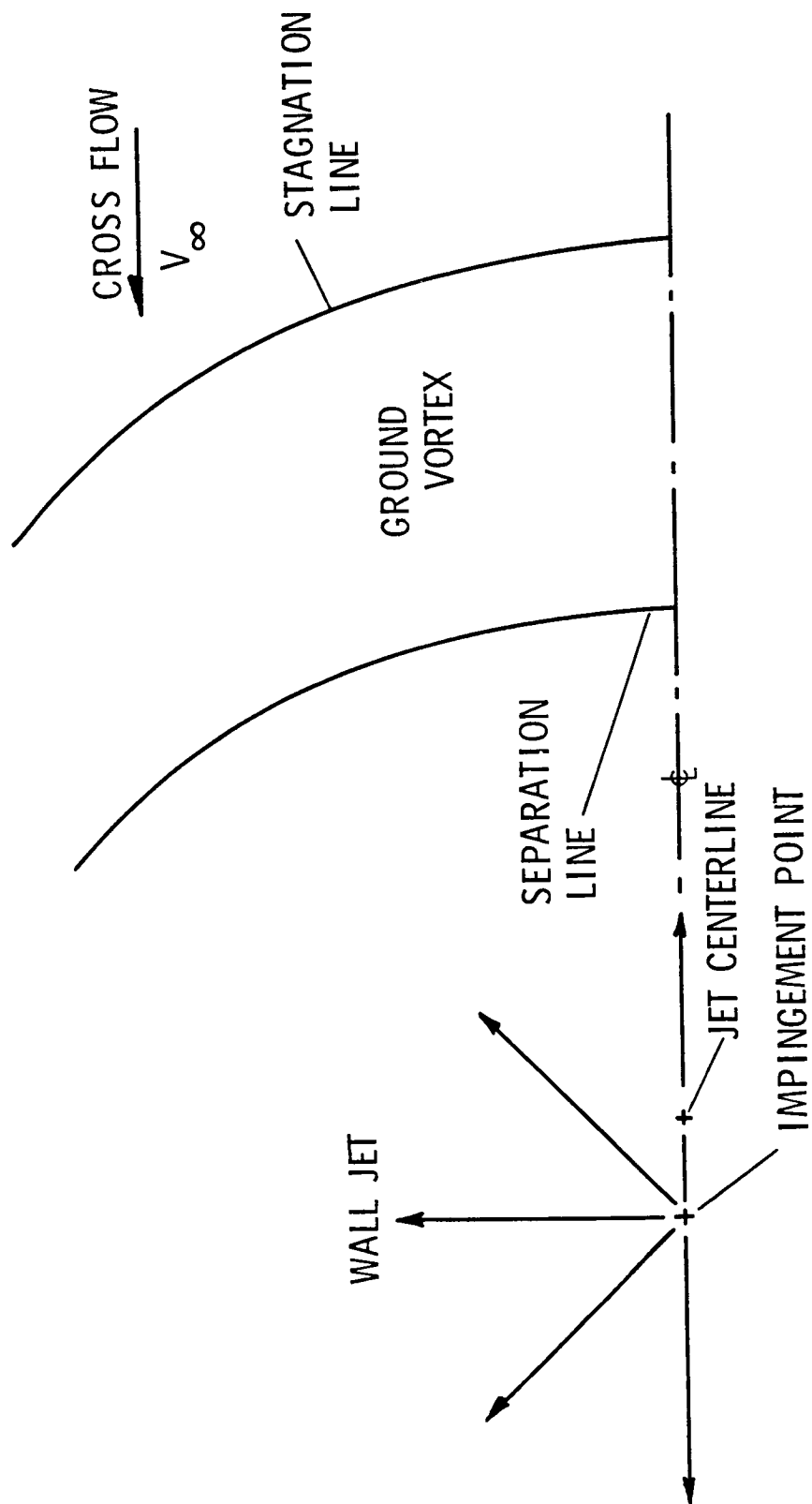
Figure 1. Top View of Ground Plane Flow Pattern
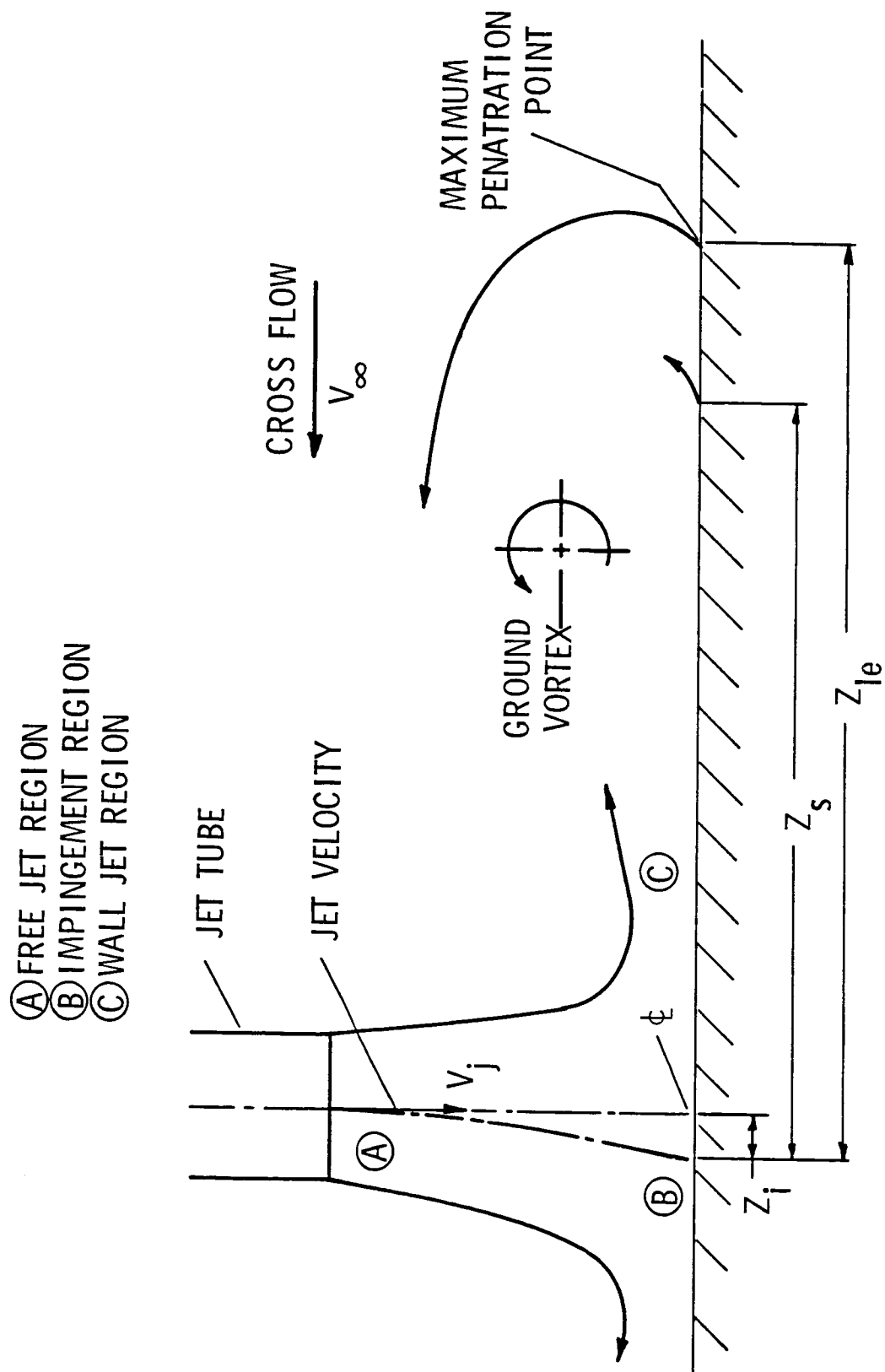
Figure 2. Vortex Formed by a Jet Impinging Normally on a Flat Plate in a Cross Flow
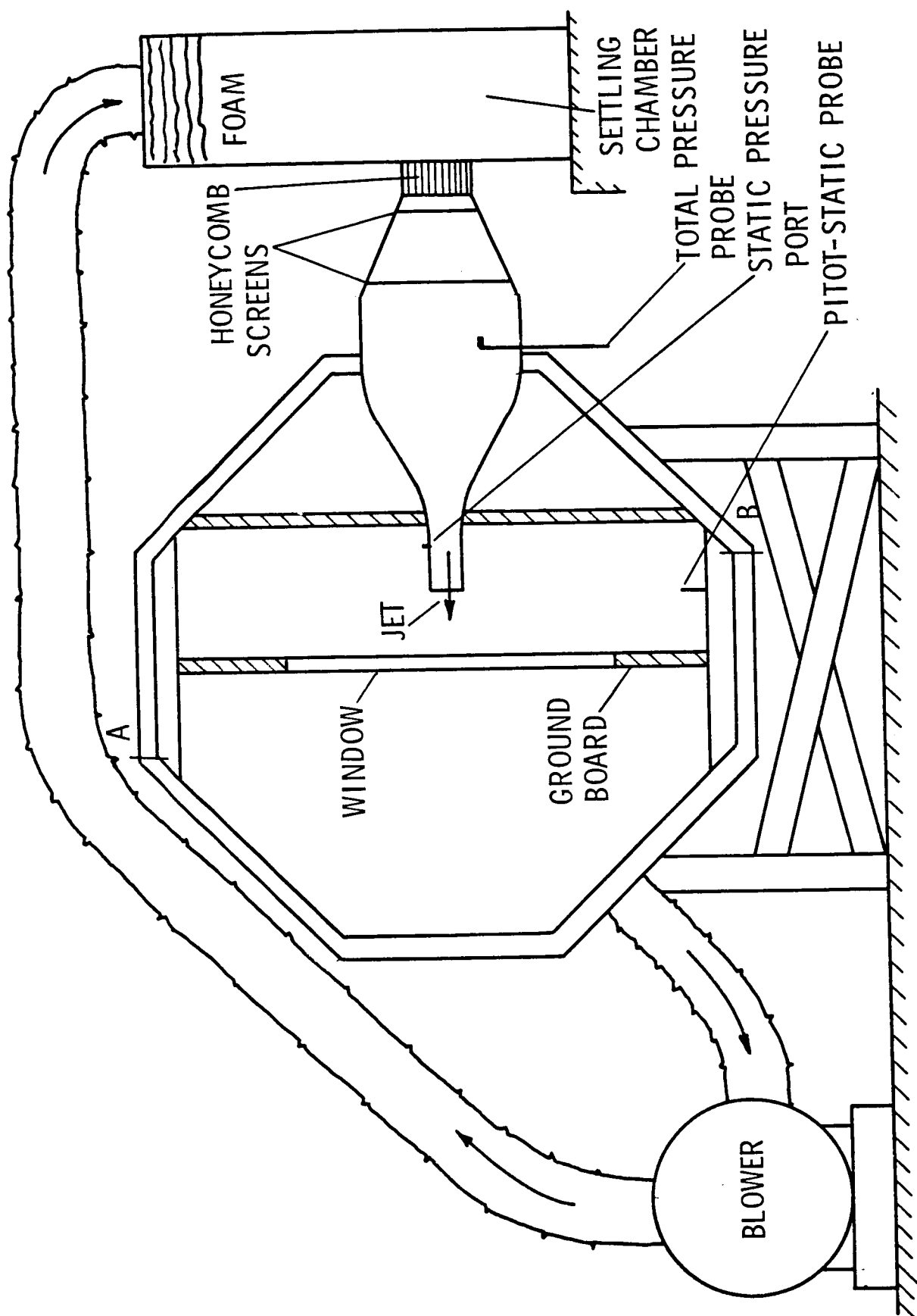
Figure 3. Jet Installation in Wind Tunnel

SECTION AA'

BOUNDARY LAYER CONTROL SLOT

INTERCHANGEABLE
WINDOW

A'

A
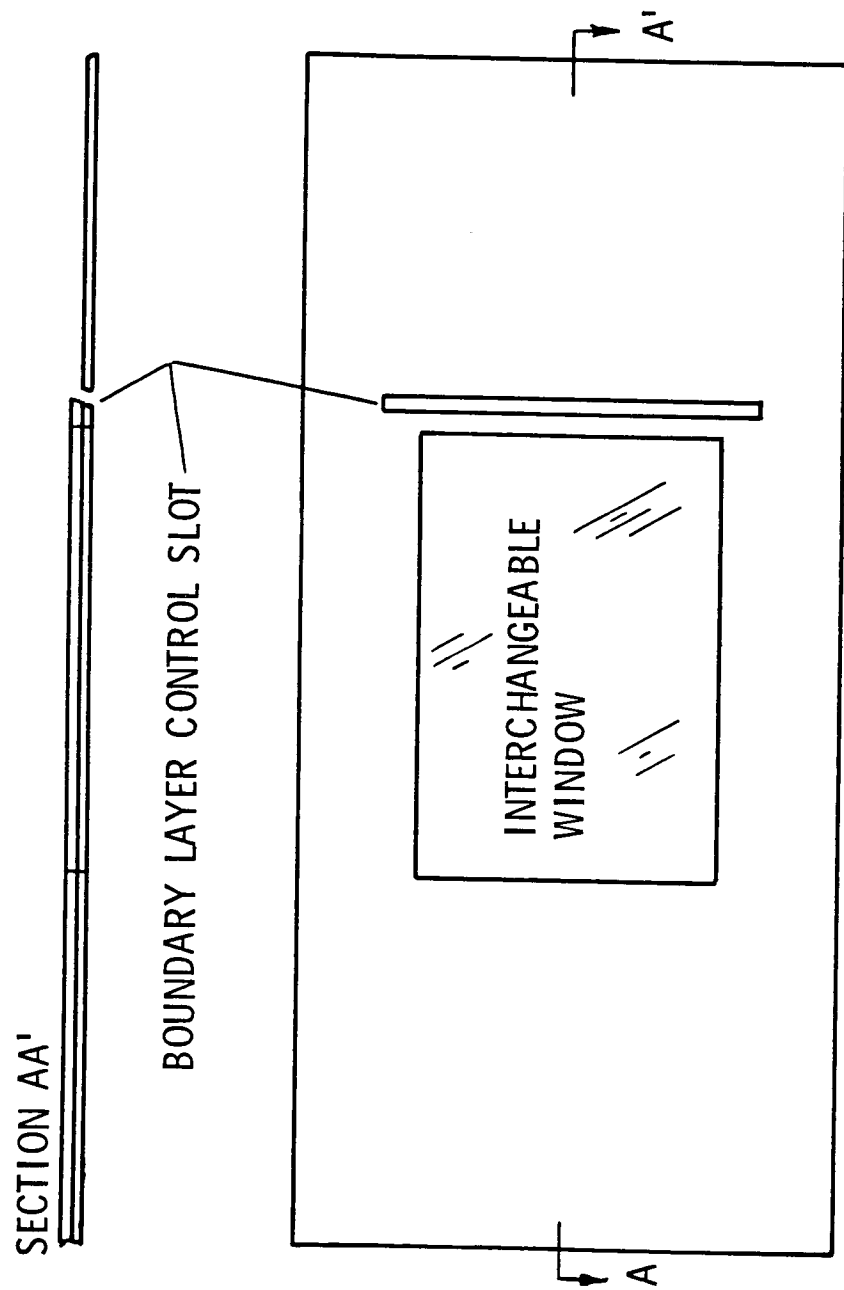
Figure 4. Ground Plane Configuration
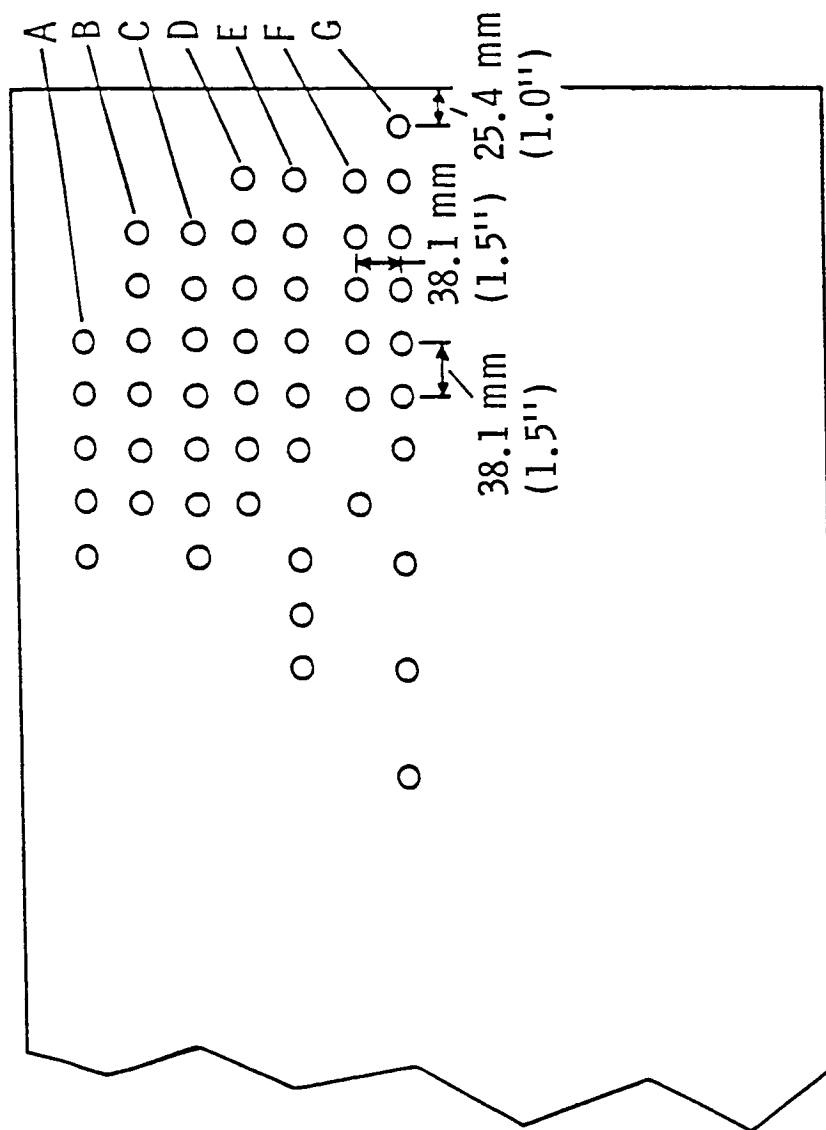
Figure 5. Pressure Window
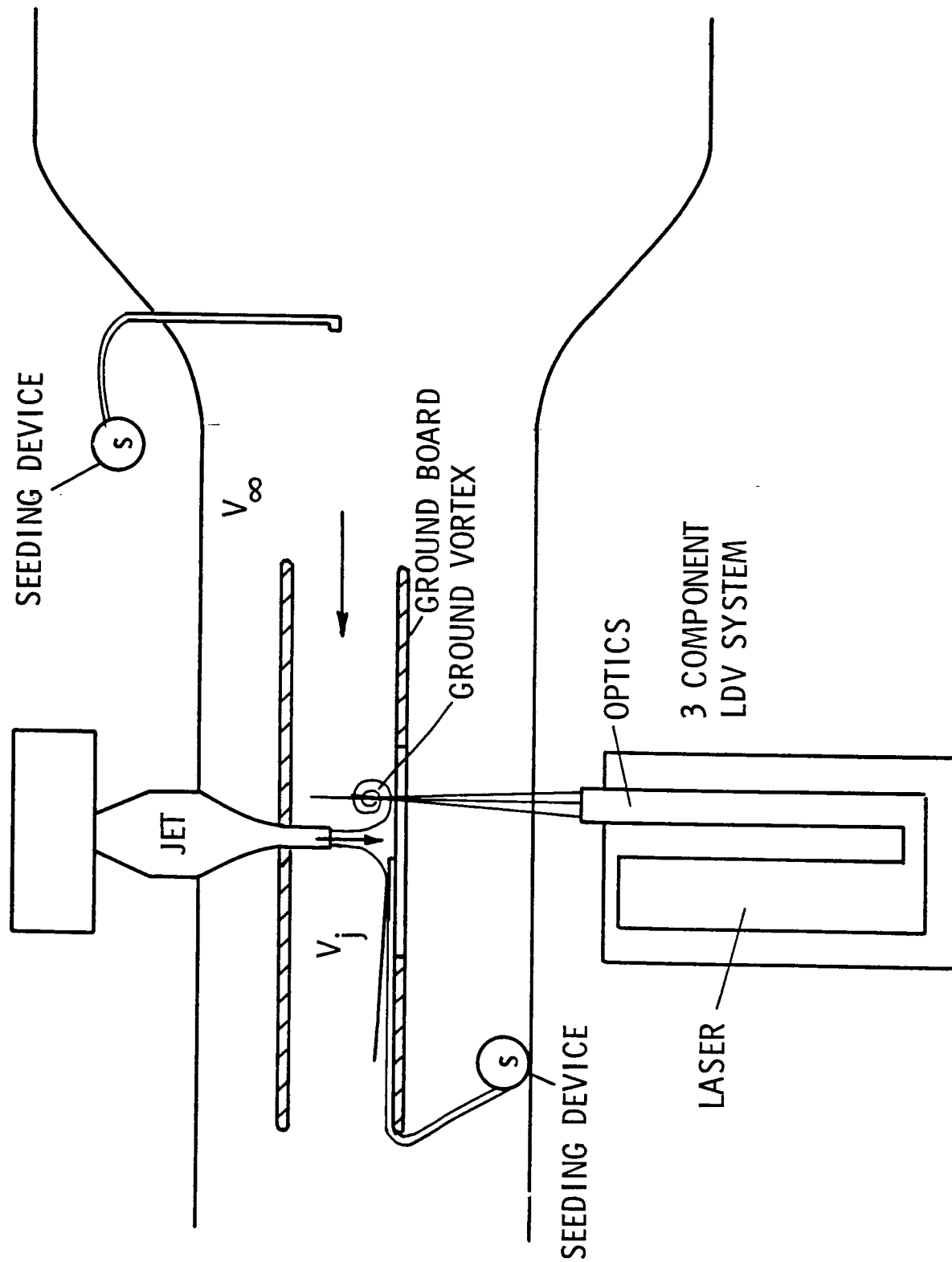
Figure 6. Laser Installation

Figure 7. Jet Characteristics -- Velocity Surveys

JET CHARACTERISTICS
TURBULENCE SURVEYS IN THE
VERTICAL PLANE AT THE JET
CENTERLINE AND AT $X/D_j = 2.0$

$V_{\mathbb{C}} = 45.7$ m/s (150 FPS)

$P_A = 97909$ Pa (14.2 PSIA)

ABOVE JET $\mathbb{C}$ ← → BELOW JET $\mathbb{C}$

JET EXIT

$D_j = 76.2$ mm (3.00")

VERTICAL POSITION RATIO: (y/D_j)

-1.0   -0.5   0   0.5   1.0

TURBULENCE INTENSITY RATIO $(T.I./T.I._{\mathbb{C}})$
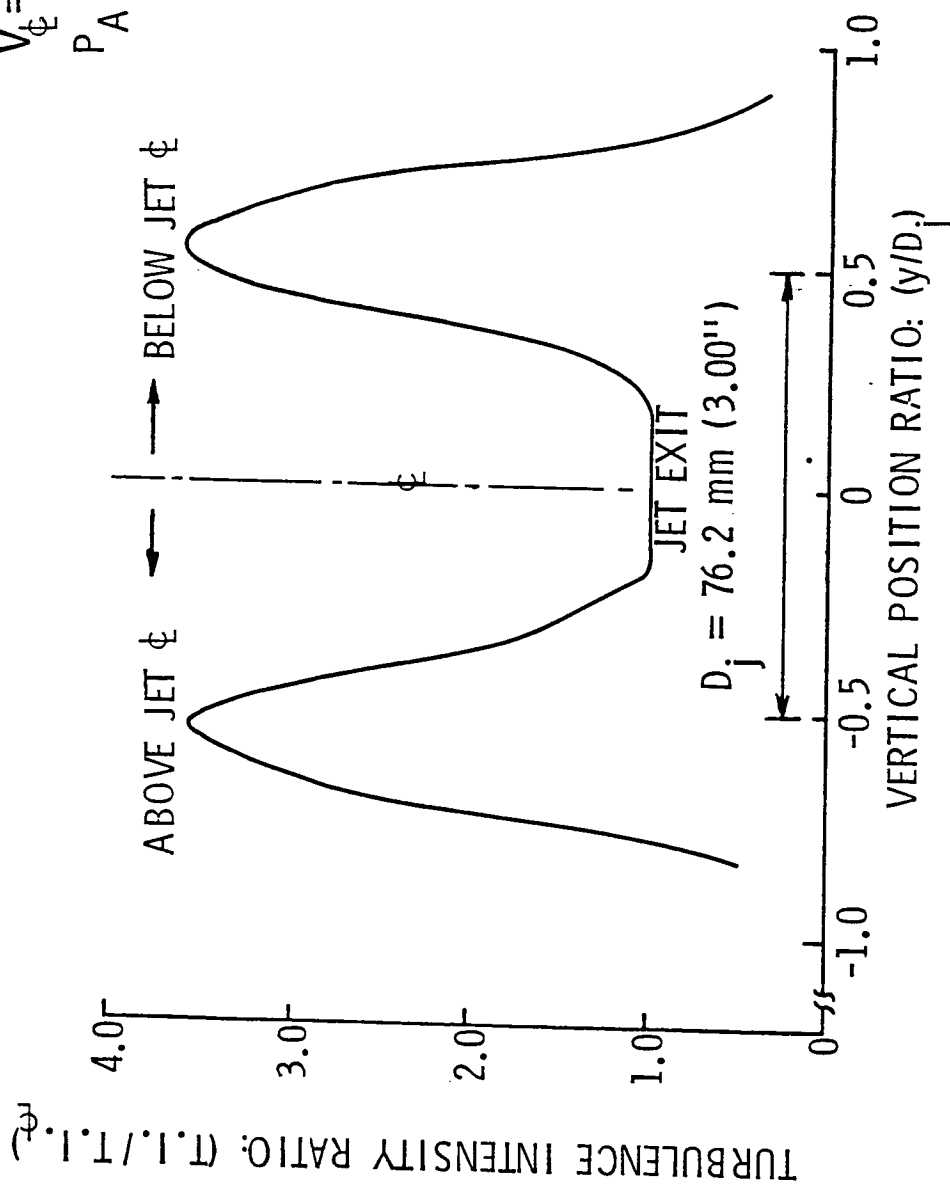
0   1.0   2.0   3.0   4.0

Figure 8.   Jet Characteristics -- Turbulence Surveys
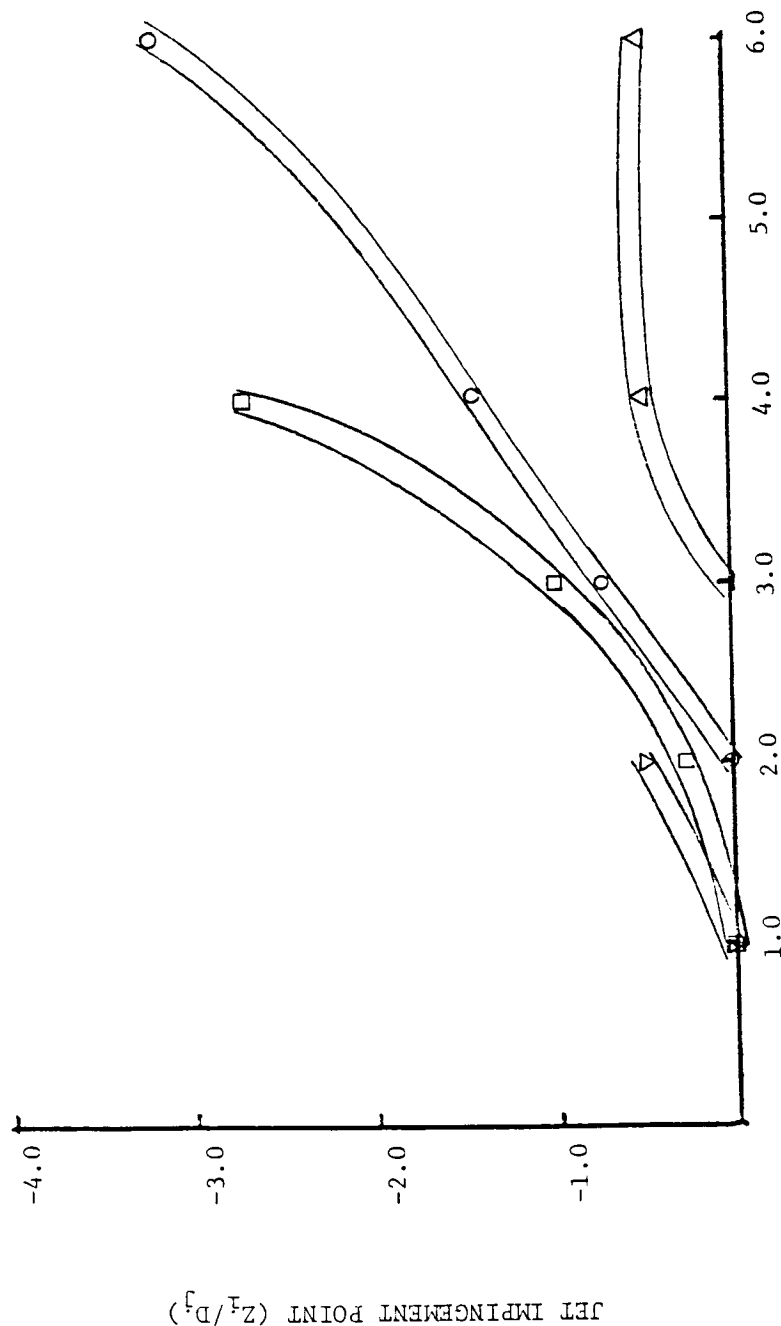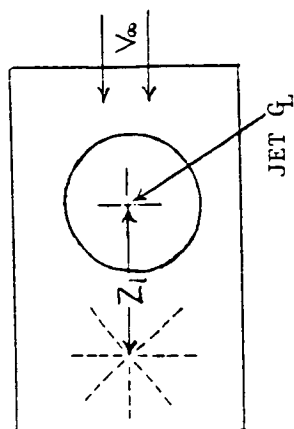
Figure 9. Variation of Jet Impingement Point With Ground Plane Location
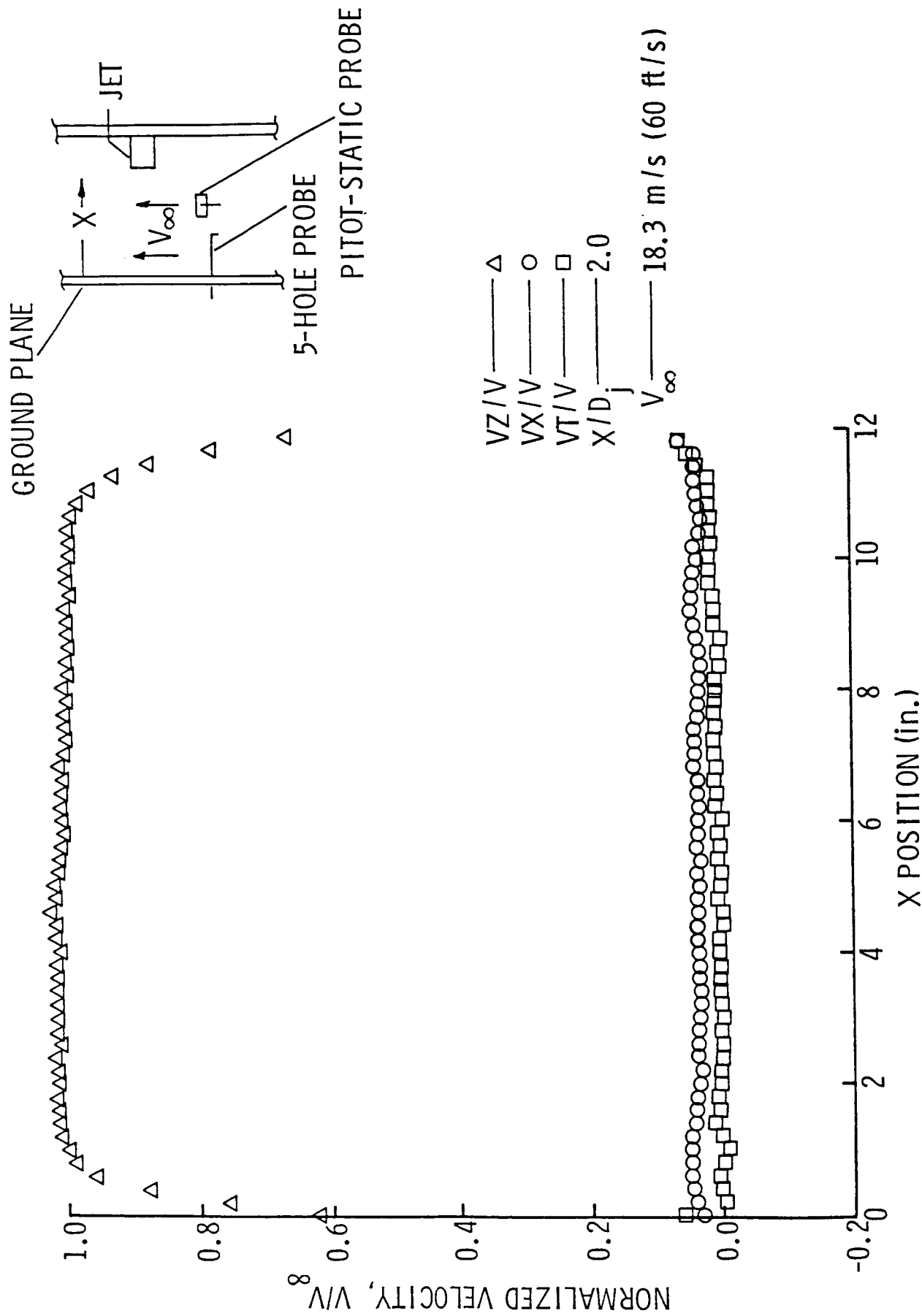
Figure 10. Test Section Velocity Surveys – $\dfrac{2Cps}{2x} < .006$
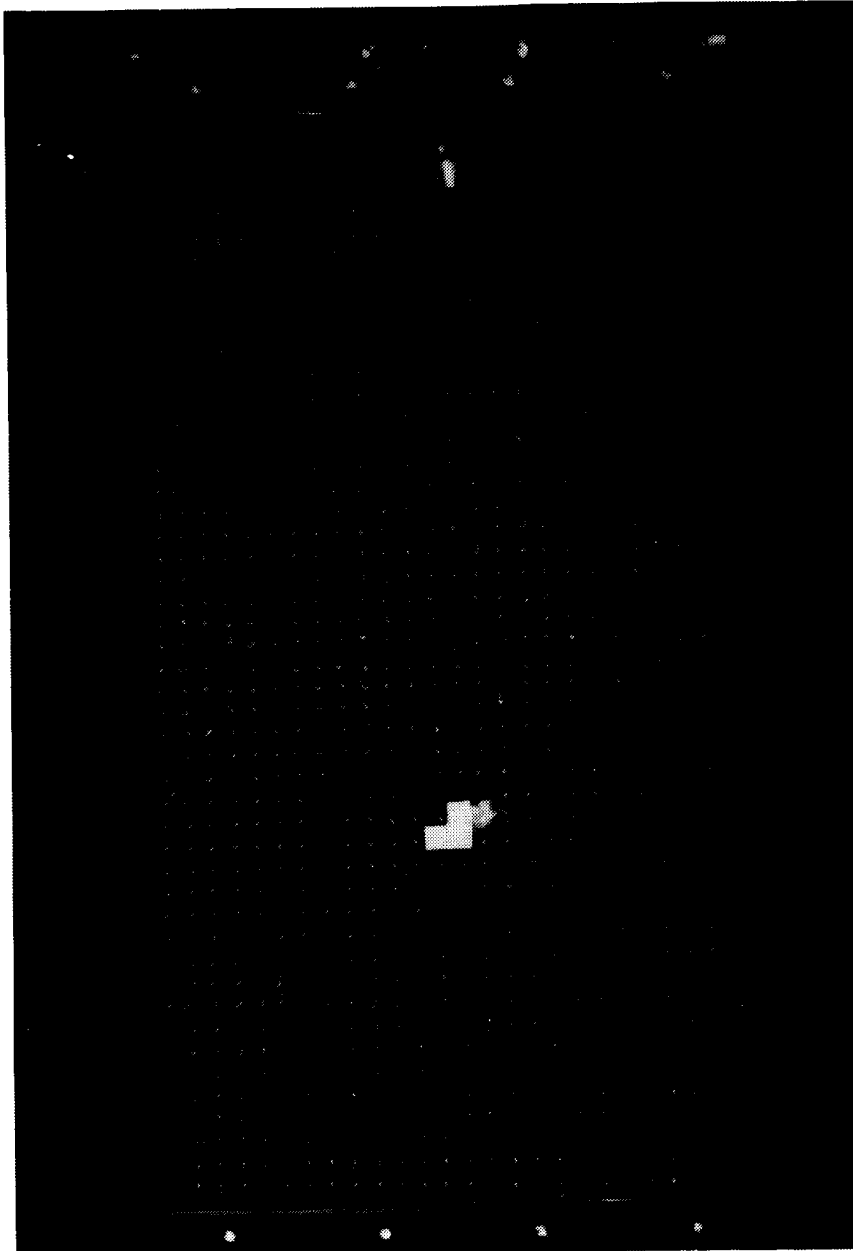
Figure 12. FLOW VISUALIZATION (X/Dj = 3.0; V_∞/V_j = 0.1)

Figure 11. Flow Visualization – Mini Tufts $(X/D_j = 2.0; V_\infty/V_j = 0.3)$
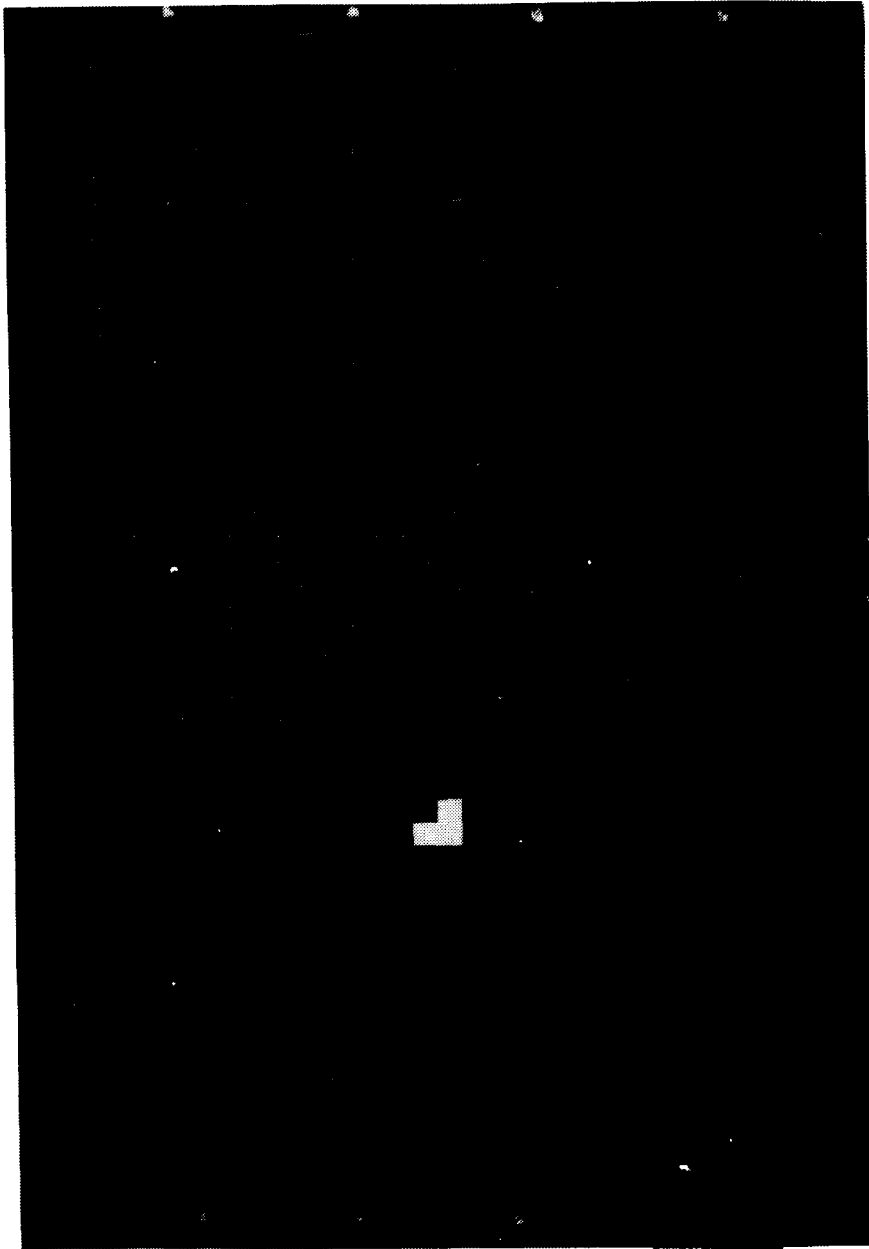
Figure 13. FLOW VISUALIZATION $(X/D_j = 3.0; V_\infty/V_j = 0.2)$
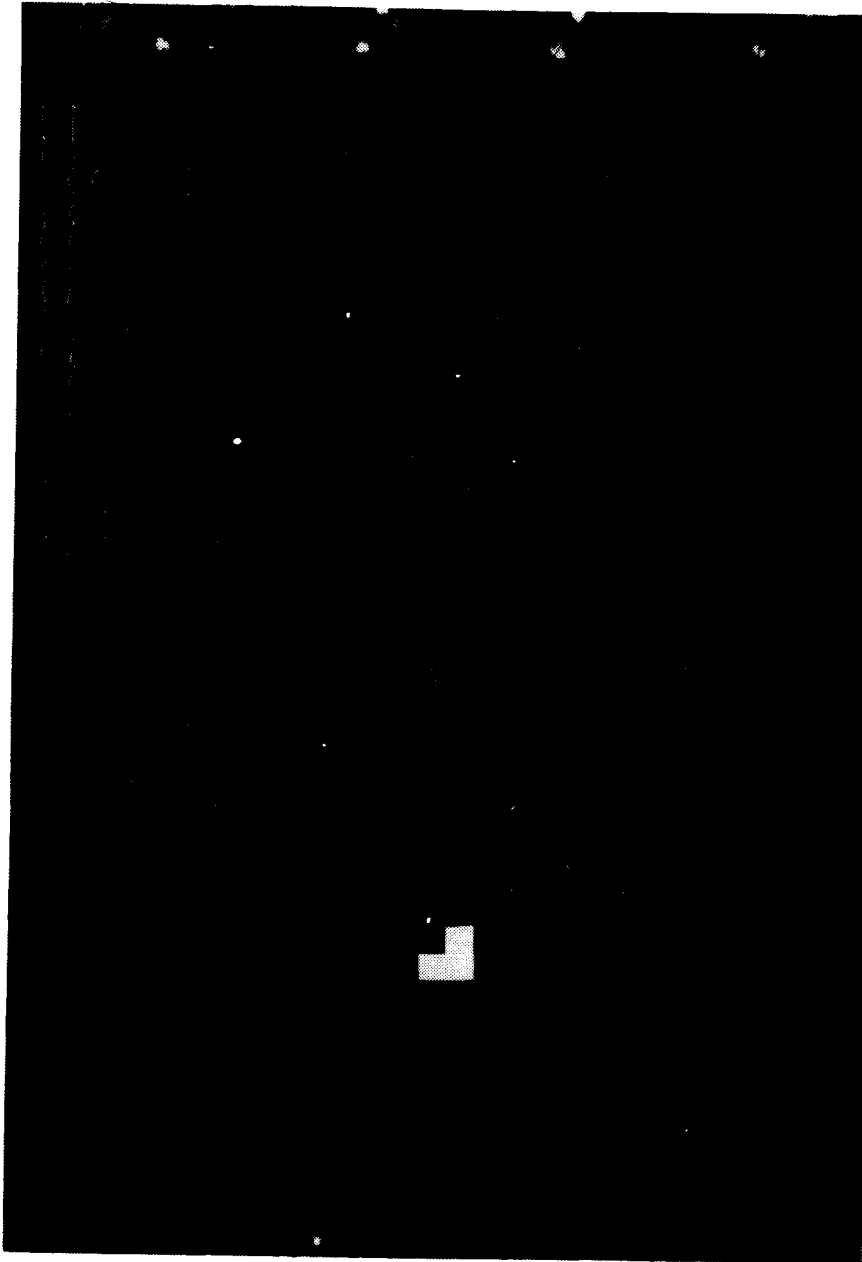
Figure 14. FLOW VISUALIZATION $(X/D_j = 3.0; V_\infty/V_j = 0.3)$
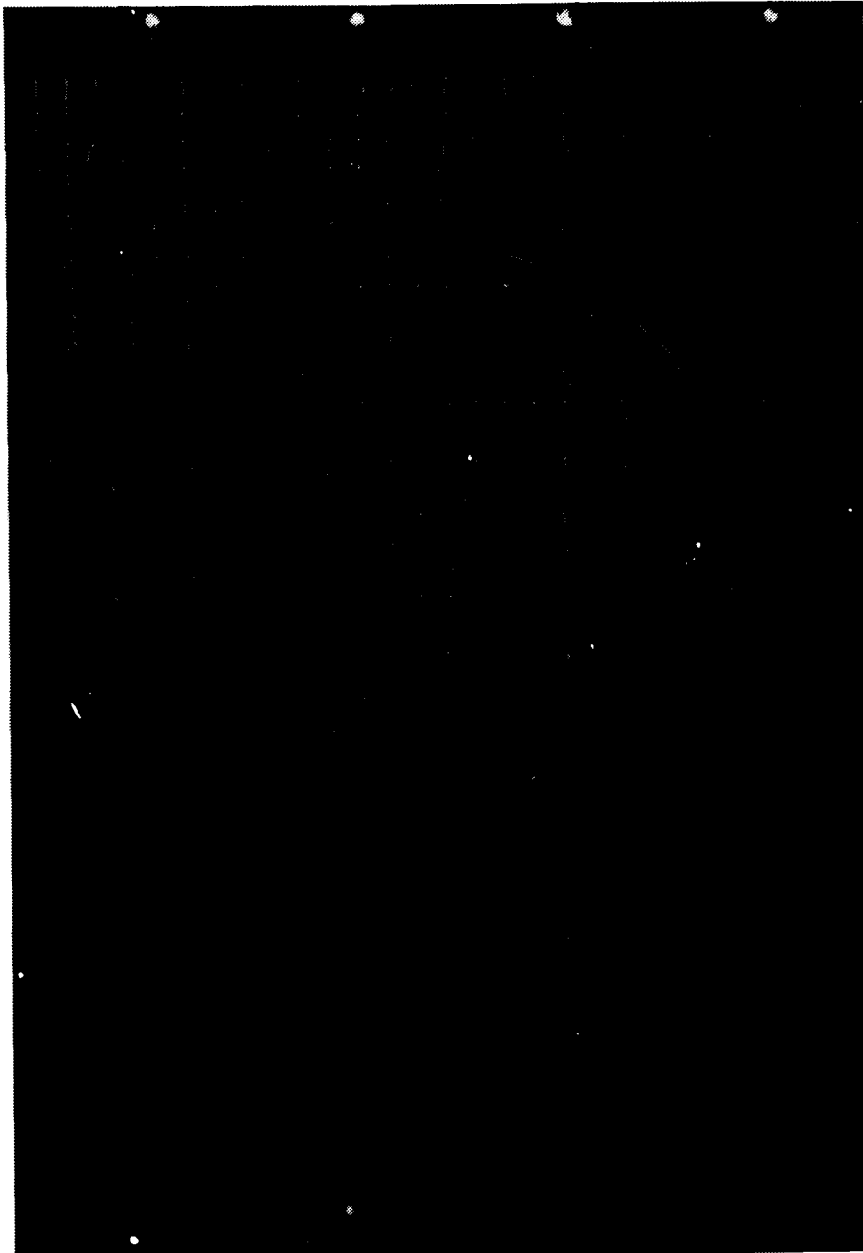
Figure 15. FLOW VISUALIZATION ($X/D_j = 3.0$; $V_\infty/V_j = 0.4$)
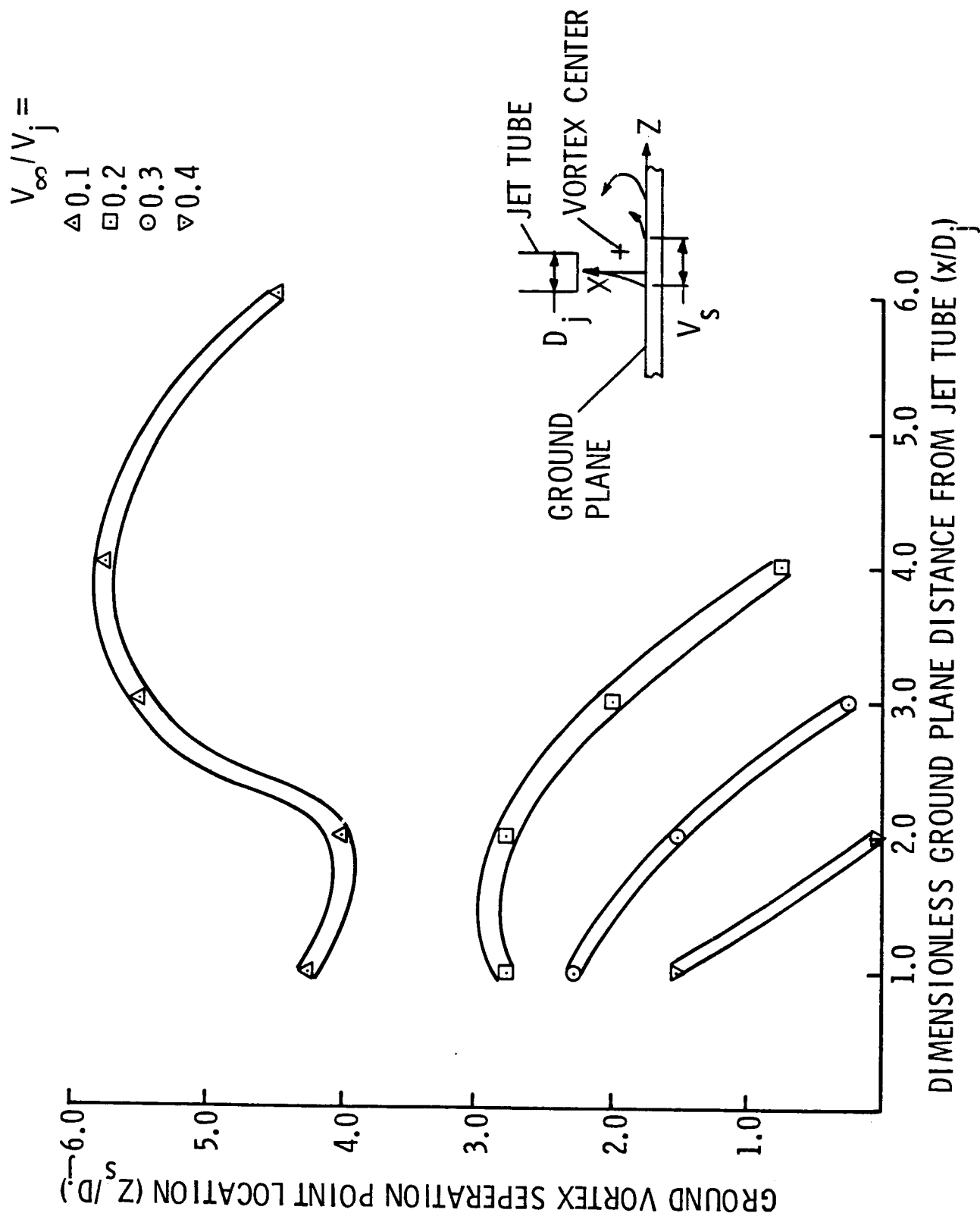
Figure 16. Variation of Ground Vortex Separation Point with Ground Plane-to-Jet Distance
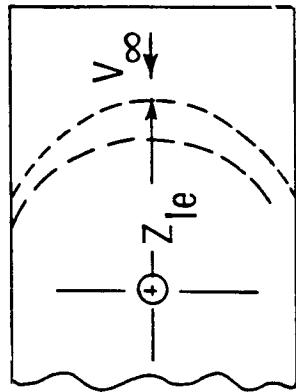
GROUND VORTEX LOCATION FROM
FLOW VISUALIZATION STUDIES AT
VARIOUS GROUND-PLANE LOCATIONS
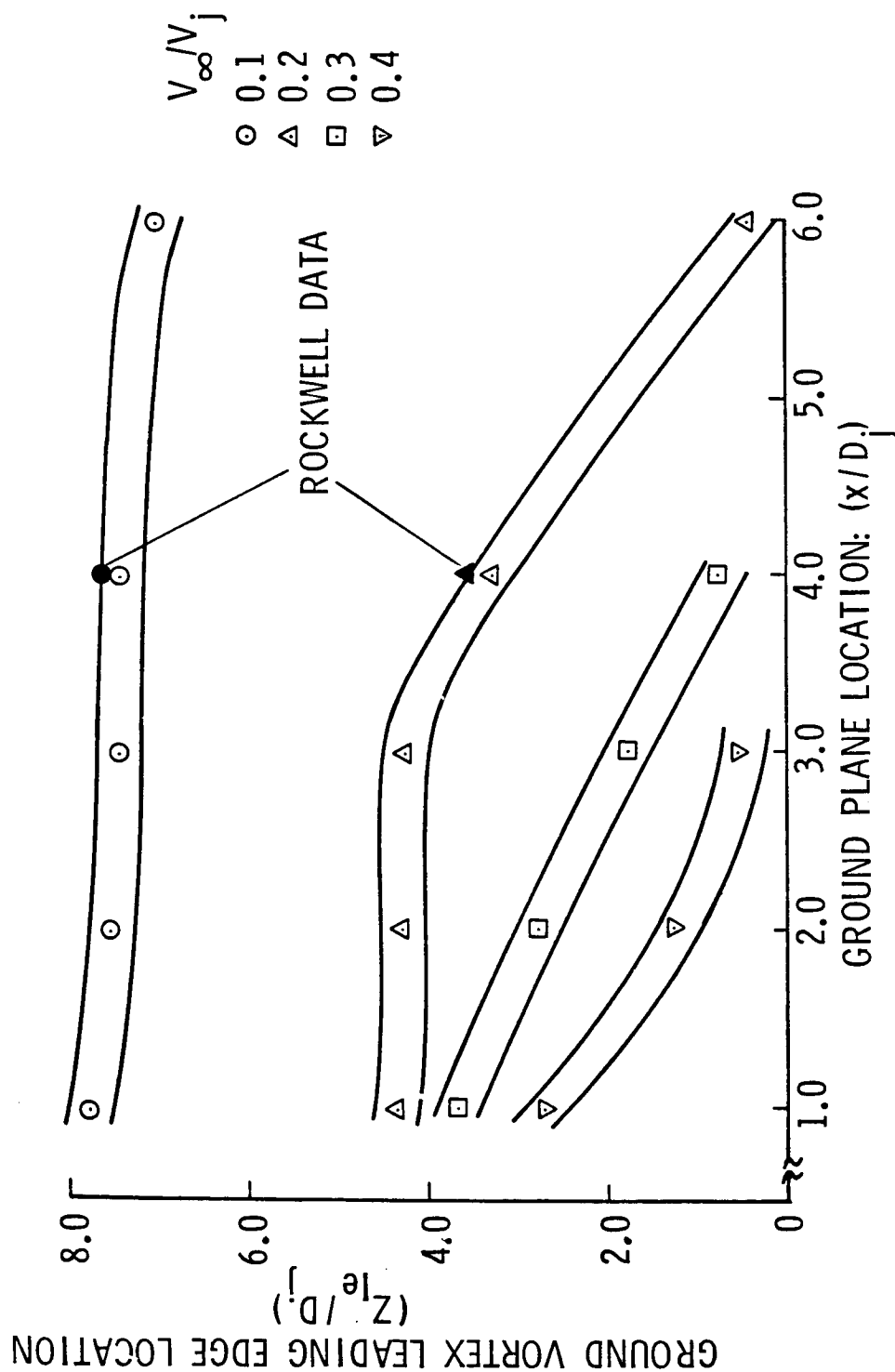
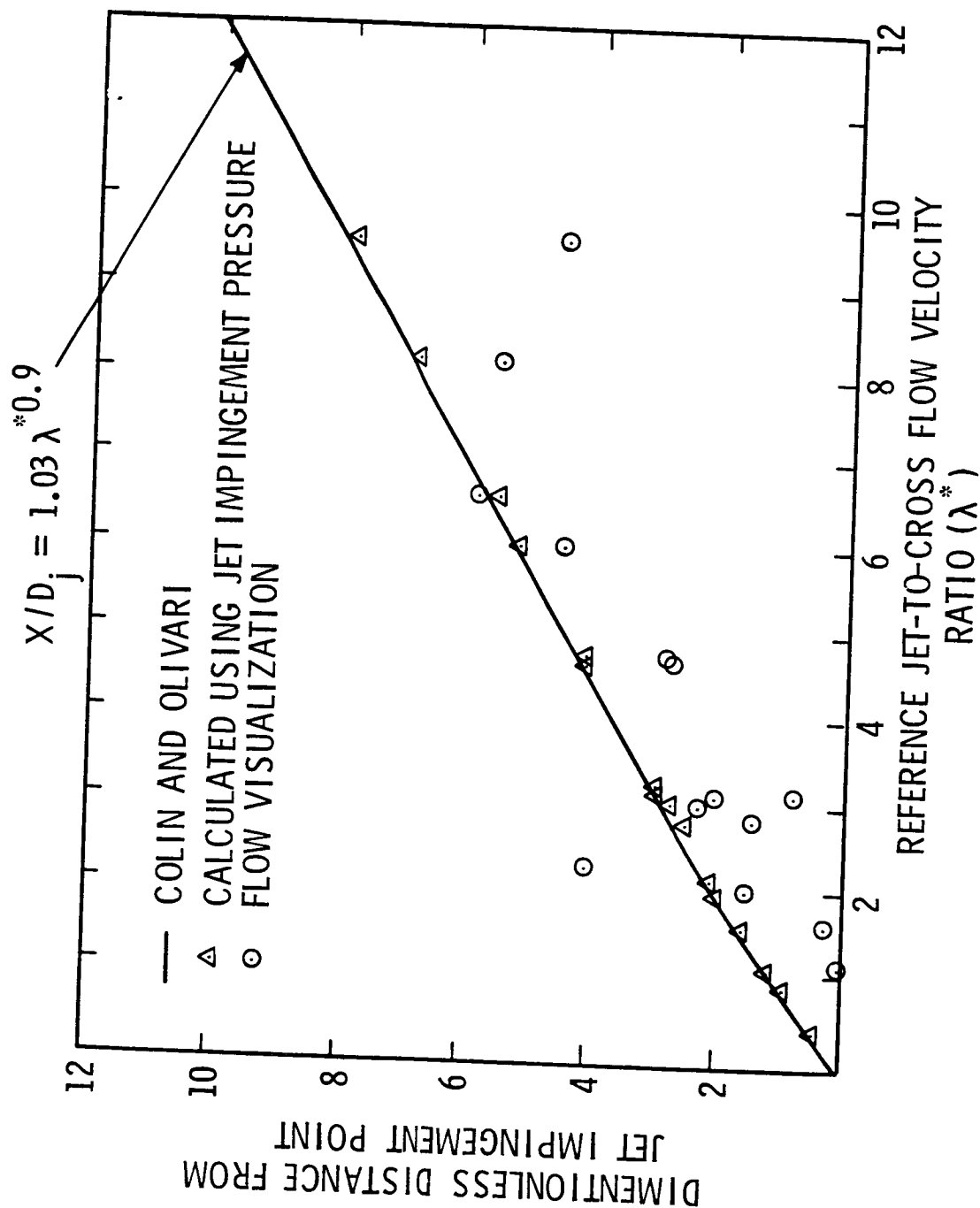Figure 17. Ground Vortex Leading Edge Location from Flow Visualization

Figure 18. Variation of Ground Vortex Separation Point with Reference
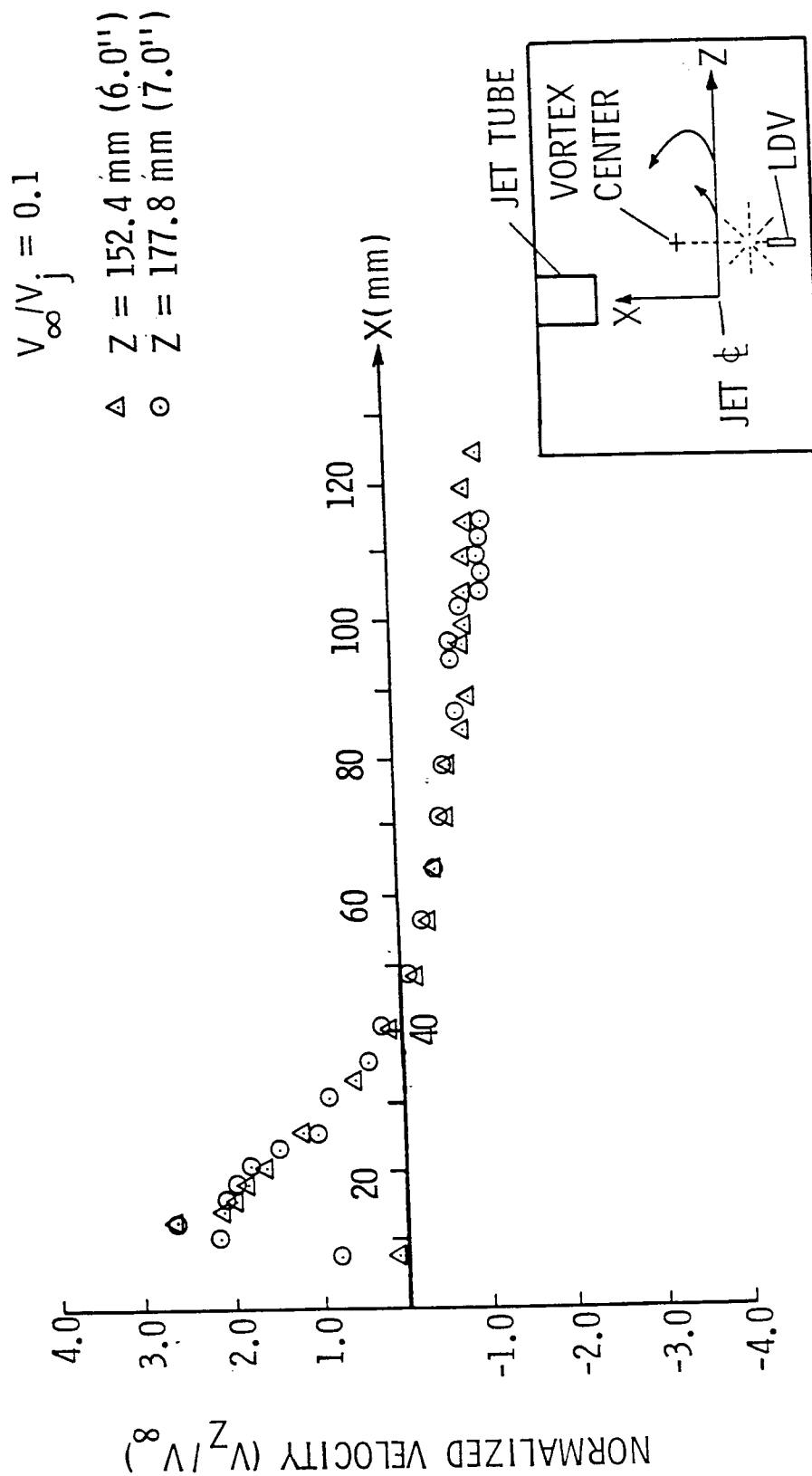Jet-to-Cross Flow Velocity Ratio

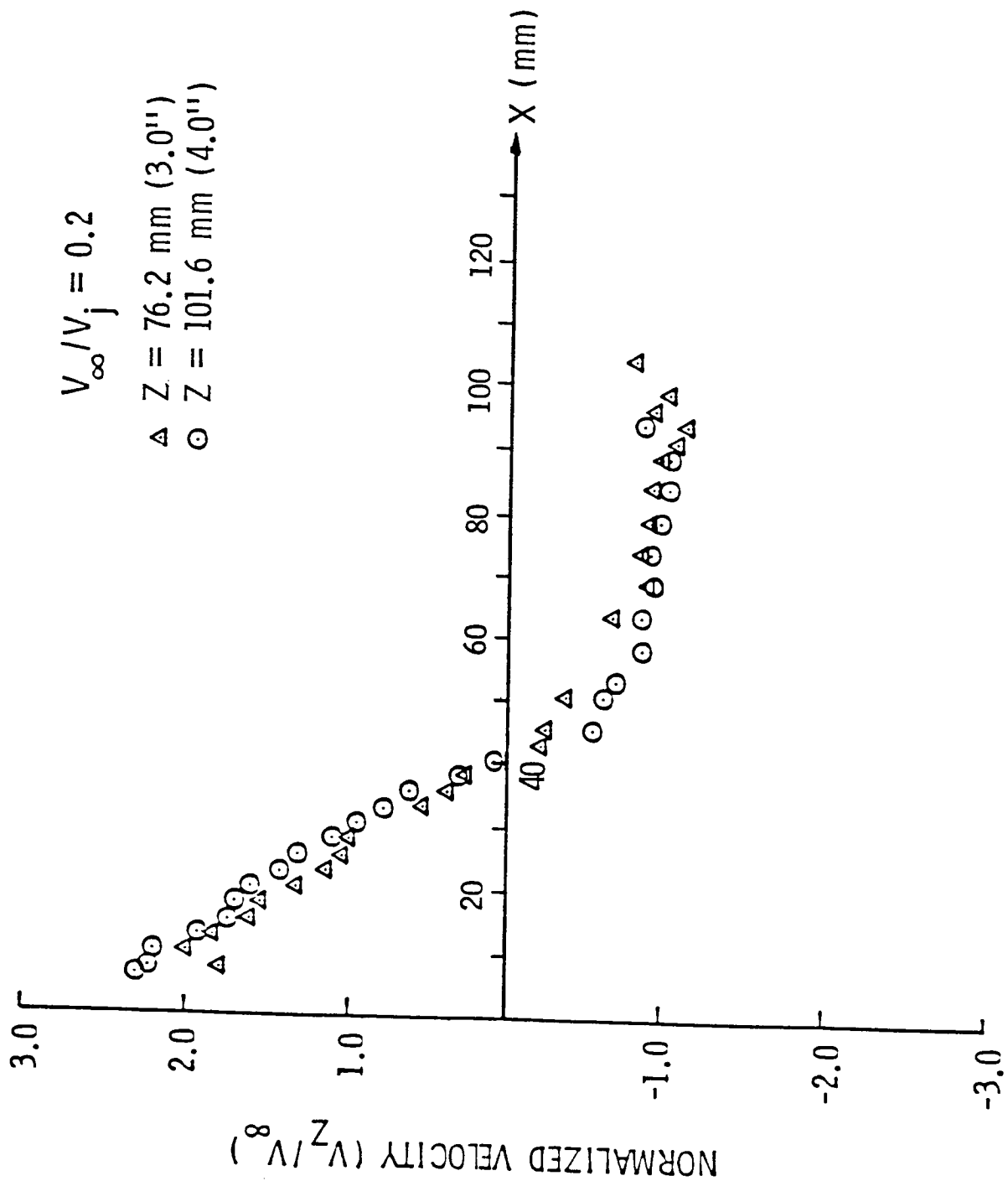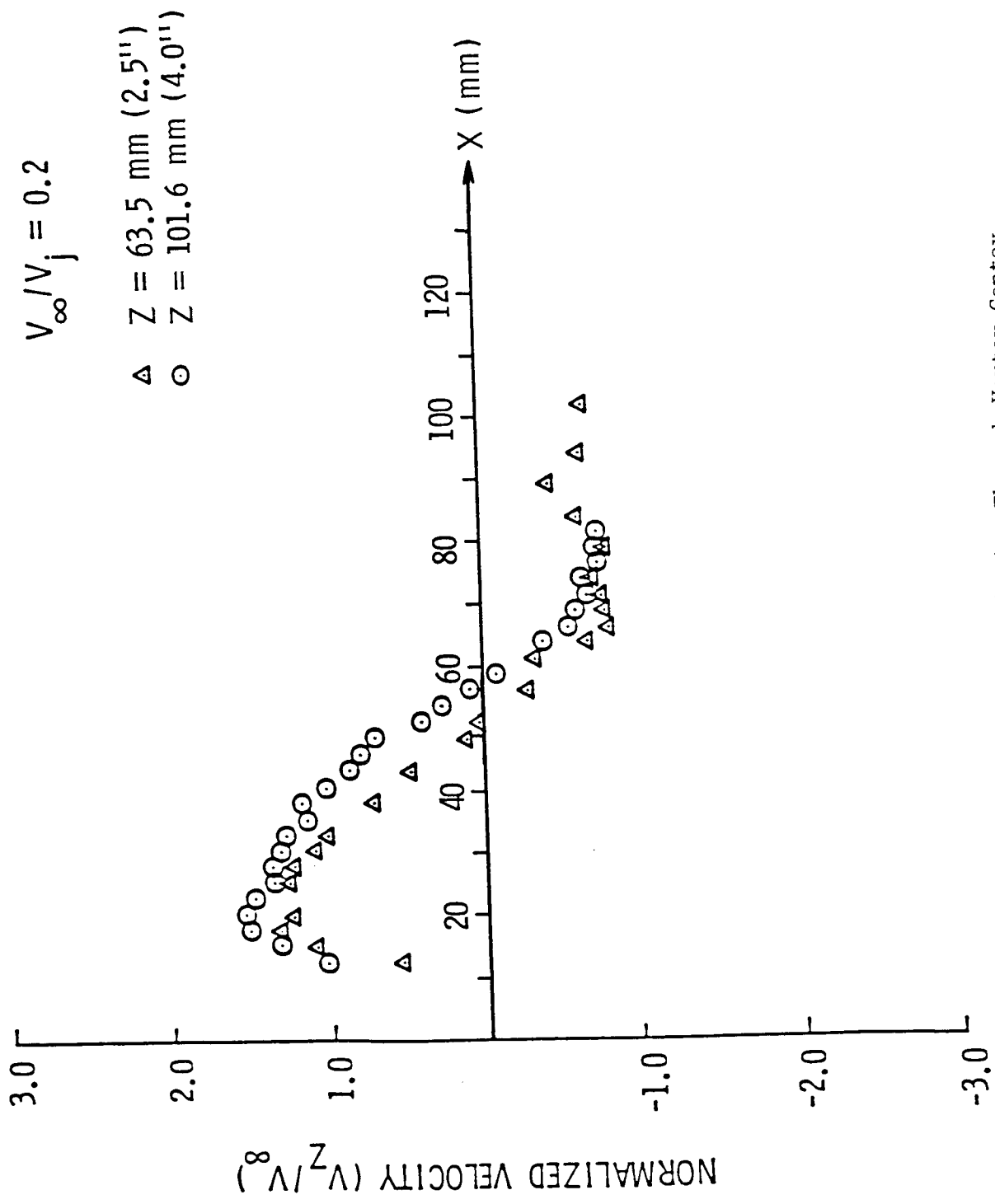Figure 19. Velocity Distribution Through Vortex Centex

236

Figure 20.   Velocity Distribution Through Vortex Center

Figure 21. Velocity Distribution Through Vortex Center

238